

# Path towards the extraction of the scattering amplitude through angular asymmetries in TCS

Rafayel Paremuzyan

April 3, 2019

This document describes proposed steps towards the extraction of the real part of the helicity conserving scattering amplitude  $Re\tilde{M}^{--}$  (look [1] for details) for the Timelike Compton scattering (TCS) process. Discussions in this note are based on studies which are presented in a workshop at Bochum in Feb 2014 [2]. At the time of this studies the CLAS12 reconstruction software was not ready, and therefore acceptance and resolution effects were studied using the CLAS12 FASTMC package. It is also discussed here the selection of kinematic points assuming 120 days of beam time with  $10^{35}cm^{-2}s^{-1}$  luminosity electron beam. Unfortunately all the codes and data files are lost, therefore almost all plots in this document will be snippets from above mentioned slides [2].

## 1 Accessing the scattering amplitude

Experimentally TCS is accessible through  $\gamma p \rightarrow e^- e^+ p$  reaction. Main contributions to this reaction are the Bethe Heitler (BH), TCS and their interference term.

$$\sigma(\gamma p \rightarrow e^- e^+ p) = \sigma_{TCS} + \sigma_{BH} + \sigma_{Int} \quad (1)$$

As discussed in [1], the TCS cross-section is very small (Fig. 10 of [1]) wrt BH cross-section, therefore in the following discussion the TCS part will be neglected. From remaining terms, BH is well known (calculable within 1%-2% precision). The interference term (eq.30 from [1]) can be represented in a following way.

$$\sigma_{Int} = a \cdot M^{--} \cdot \frac{L_0(\theta)}{L(\theta, \phi)} \cdot \cos(\phi) \quad (2)$$

where

$$a = -\frac{\alpha_{em}^3}{4\pi s^2} \frac{1}{-t} \frac{M}{Q'} \frac{1}{\tau\sqrt{1-\tau}} \frac{1 + \cos^2(\theta)}{\sin(\theta)} \quad (3)$$

As in the paper [1], here too, we will use the weighted cross section (WCRS),  $\frac{dS}{dQ'^2 dtd\phi}$ , which is obtained from the differential cross section  $\frac{d\sigma}{dQ'^2 dtd(\cos(\theta))d\phi}$  weighted by  $\frac{L}{L_0}$  and integrated over  $\theta$  (in [1] from  $\pi/4$  to  $3\pi/4$ ). The main reason for not integrating over the whole  $\theta$  range (0 to  $\pi$ ) is because BH dominates over the interference term at  $\theta \sim 0^\circ$  and  $\theta \sim 180^\circ$  (the  $\frac{\sigma_{BH}}{\sigma_{int}} \sim \frac{1}{\sin(\theta)}$ ). The exact values of integration limits is a subject for studies, and these limits must be chosen to minimize uncertainties on the extracted scattering amplitude  $M^{--}$ .

26 The WCRS has the following shape

$$\frac{dS_{Tot}}{dQ^2 dtd\phi} = \int_{\pi/4}^{3\pi/4} d\theta \frac{d\sigma}{dQ^2 dtd(\cos(\theta)) d\phi} = S_{BH} + S_{Int} = S_{BH} + A \cdot ReM^{--} \cdot \cos(\phi) \quad (4)$$

27 Here  $A = \int_{\pi/4}^{3\pi/4} d\theta \cdot a = -\frac{\alpha_{em}^3}{4\pi s^2} \frac{1}{-t} \frac{M}{Q'} \frac{1}{\tau \sqrt{1-\tau}} \int_{\pi/4}^{3\pi/4} (1 + \cos^2(\theta)) d\theta$

28 Now, if one subtracts the weighted BH cross section from the total weighted cross section, then the  
 29 result will be the weighted interference term which has a cosine dependence on the angle  $\phi$ . With this  
 30 proposed method we should divide the  $\phi \in (0, -2\pi)$  range into  $N_\phi$  bins ( $N_\phi$  to be determined), and for  
 31 each  $\phi$  bin subtract calculated weighted BH cross section from the measured total weighted cross section.  
 32 The resulting distribution should have a cosine dependence on the angle  $\phi$ , moreover the amplitude of  
 33 the modulation is proportional to the scattering amplitude  $ReM^{--}$ . In order to extract the  $ReM^{--}$ , this  
 34 distribution should be fitted with a function

$$f = P \cdot \cos(\phi) \quad (5)$$

35 As an example the plot in Fig.1 is an illustration of a similar fit. Points in the plot are not real data  
 36 points, but they were generated using a Gaussian function with the mean equal to the weighted cross  
 37 section in a given kinematic bin ( $t, Q^2, \phi$ ), and sigma equal to the statistical uncertainty (estimated using  
 CLAS12 FASTMC) of the cross section in the given bin. As soon the parameter  $P$  will be extracted from

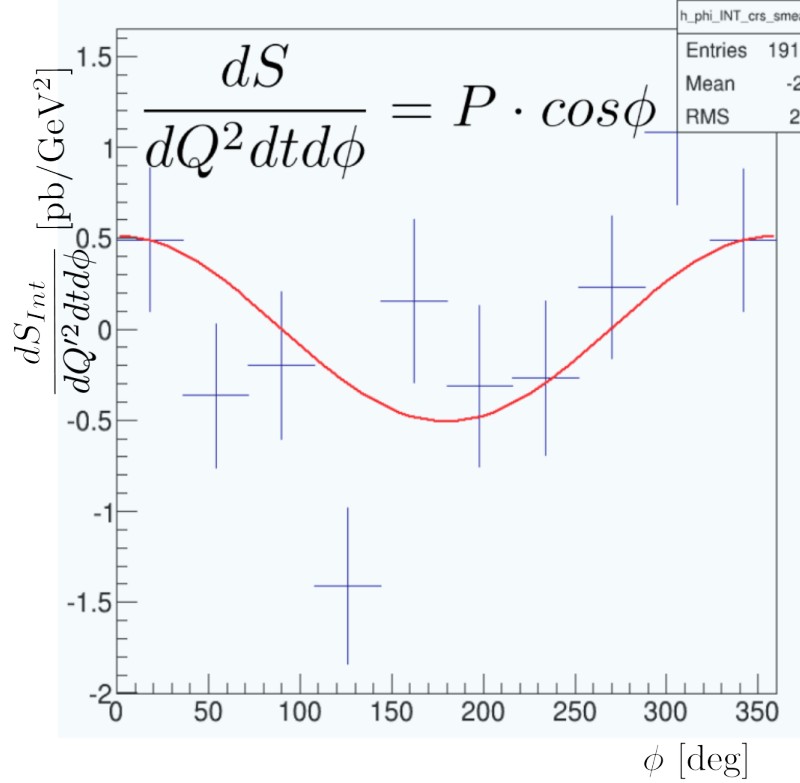


Figure 1: Illustration plot: The  $\phi$  angular dependence of the weighted interference term cross section is fitted with cosine function.

38 the fit, one then can calculate the real part of  $M^{--}$   
 39

$$ReM^{--} = -\frac{P}{\frac{\alpha_{em}^3}{4\pi s^2} \cdot \frac{1}{-t} \frac{M}{Q'} \frac{1}{\tau \sqrt{1-\tau}} \int_{\pi/4}^{3\pi/4} (1 + \cos^2(\theta)) d\theta} \quad (6)$$

## 2 The Effect of the CLAS(12) acceptance and the extrapolation

It is important to mention that in the above described method, integration limits over  $\theta$ , should not be changed for different  $\phi$  bins. Varying integration limits, the  $\phi$  dependence of the weighted cross section will not have a cosine shape anymore.

The CLAS and CLAS12 detector acceptances have strong  $\theta$  and  $\phi$  dependence. As an example in Fig.2

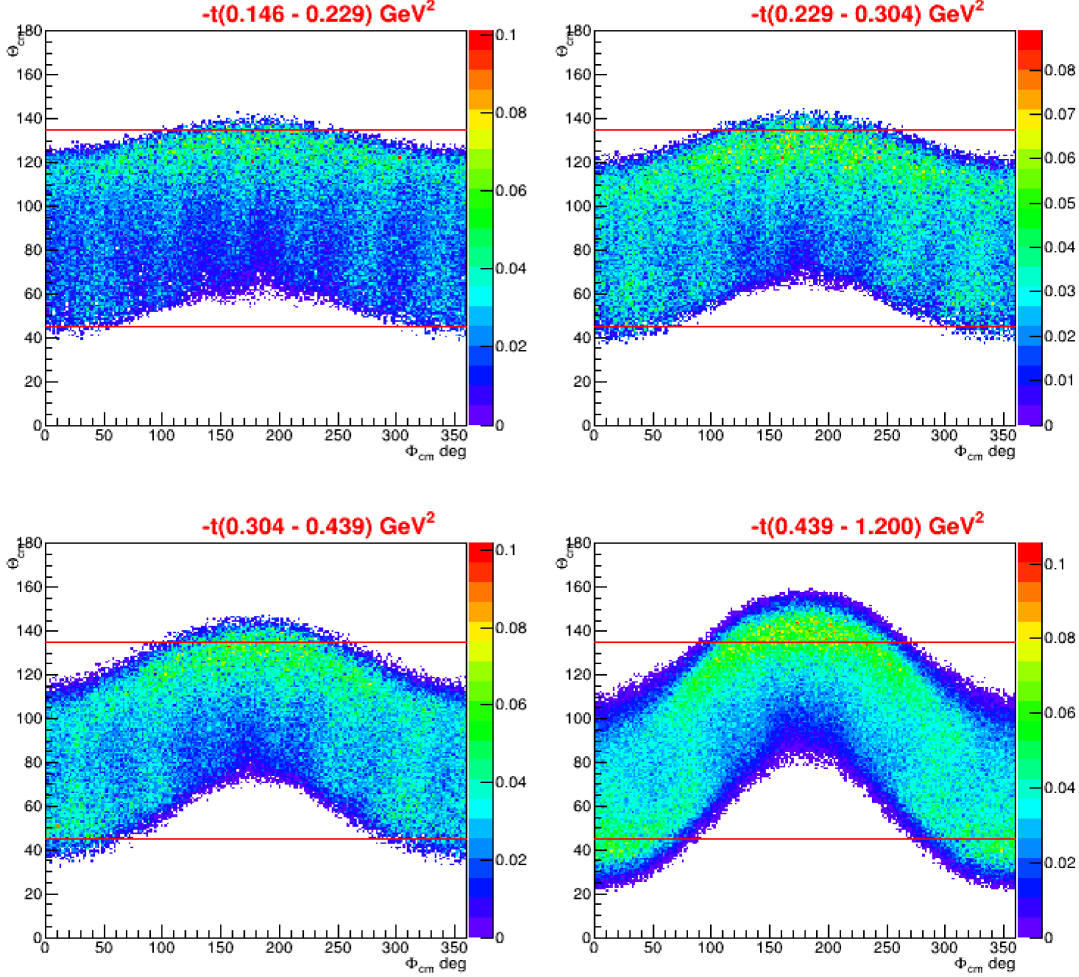


Figure 2: CLAS12 acceptance obtained in different  $-t$  bins. Acceptance are calculated through CLAS12 FASTMC package.

shown CLAS12 acceptance obtained in different  $t$  bins. One can see that the CLAS12 acceptance doesn't cover the full  $\theta$  range, and moreover, the  $\theta$  range varies a lot as a function of the angle  $\phi$ . This means that if in the data we integrate over  $\theta$  in the available  $\theta$  range, then the resulting distribution will not have a cosine dependence on the angle  $\phi$ .

Now let's look into the equation (4). It shows that the WCRS of interference term has as  $1 + \cos^2(\theta)$  dependence on the angle  $\theta$  for any angle  $\phi$ , and if one measures the interference term WCRS in a given range  $\theta \in (a, b)$ ,  ${}_a^b S_{Int}$ , then one can uniquely calculate the interference term WCRS in any  $\theta \in (A, B)$  range.

$${}_A^B S_{Int} = {}_a^b S_{Int} \frac{\int_A^B (1 + \cos^2(\theta)) d\theta}{\int_a^b (1 + \cos^2(\theta)) d\theta} \quad (7)$$

53 The interference term WCRS can be calculated by subtracting the BH WCRS from the total measured  
 54 WCRS.

$${}^b_a S_{Int} = {}^b_a S_{Tot} - {}^b_a S_{BH} \quad (8)$$

55 In short: the  ${}^b_a S_{Tot}$  will be measured from the experiment, the  ${}^b_a S_{BH}$  will be calculated by integrating the  
 56 analytic form the BH cross section over the  $\theta \in (a - b)$ , and therefore the interference term WCRS will be  
 measured using the eq. (8). Then using equations 8 and 7, the interference term WCRS will be calculated

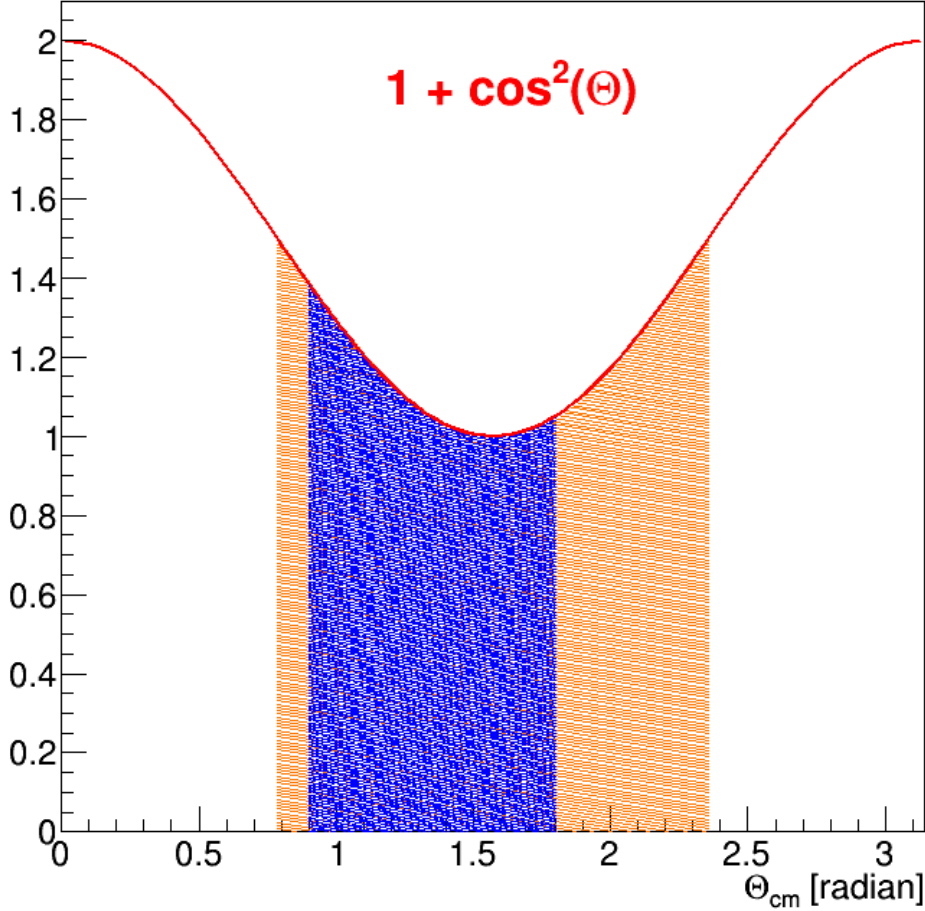


Figure 3: The interference term has a  $(1 + \cos^2(\theta))$  dependence on the angle  $\theta$ , for any  $\phi$  bin.

57 for any  $\theta \in (a - b)$  range for any given  $\phi$  bin. As an illustration, in Fig.3 shown the function  $(1 + \cos^2(\theta))$   
 58 and the integral of the 'Orange' are can be extrapolated by knowing the 'blue' shaded are by using the  
 59 equation (7). In our case the blue shaded area will correspond the CLAS(12) acceptance, and the orange  
 60 shaded area will correspond to the  $\pi/4$  to  $3\pi/4$  range.  
 61

### 62 3 estimation of statistical uncertainties

63 The statistical uncertainty on the  $ReM^{--}$  can be obtained in a following way. Let's assume the final  
 64 distribution of the interference term WCRS is the one depicted on Fig.1. Using this distribution as a  
 65 source, we will generate a big number (e.g. 10000 or more) of similar distributions, in a way that a WCRS

66 in a given  $\phi$  bin will be a Gaussian random number with a Mean equal to the WCRS and sigma equal to  
 67 the statistical error of corresponding bin of the source distribution. Then each of generated distribution  
 68 will be fitted with a cosine function in a same way as the source distribution, and each fit will yield a  
 69 certain  $ReM^{--}$ . The distribution of  $ReM^{--}$  is expected to be a Gaussian with a mean equal to the value  
 70 of  $ReM^{--}$  obtained from the source distribution, and the  $\sigma$  of it will show the statistical uncertainties  
 71 of the measured  $ReM^{--}$ . As an example the distribution in Fig.1 is actually one of such generated  
 72 distributions, and when we generated 10000 of such distributions, and fit with a  $P \cdot \cos(\phi)$  function, the  
 resulting distribution of the  $P$  is shown in Fig.4. The width of this distribution will represented the

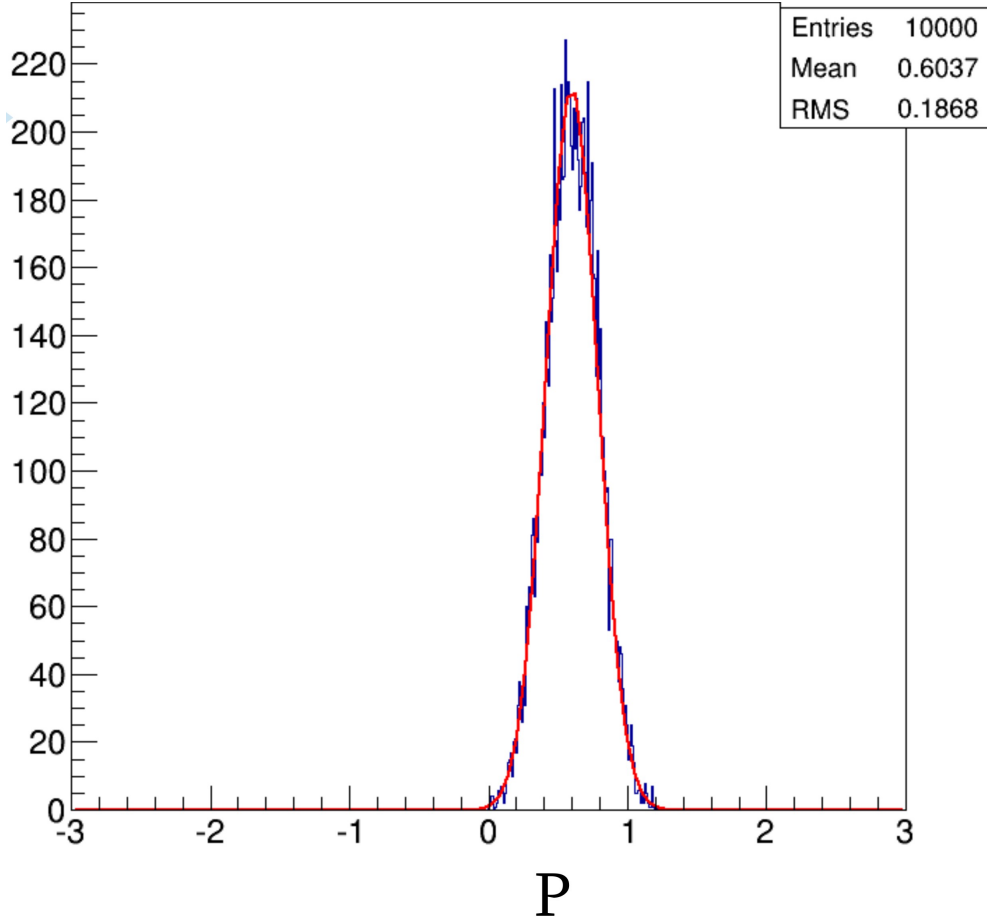


Figure 4: distribution of fit parameter  $P$  obtained from 10000 generated distributions.

73 statistical uncertainty of  $P$  which is related to  $ReM^{--}$  by eq(6).  
 74

## 4 selection of kinematic points

76 In this section we will discuss selection of TCS kinematic points, and compare TCS phase space to the  
 77 DVCS phase space which is approved for Hall-C kinematics [3]. In TCS, the corresponding variables of  
 78  $Q^2 \equiv (p_e - p_e'^2)$  and  $x_B \equiv Q^2/2pq$ , are  $Q'^2 = M_{e^-e^+}^2$  and  $\tau = Q'^2/2pq$ . In Fig.5 shown the  $Q^2$  vs  $x_B$



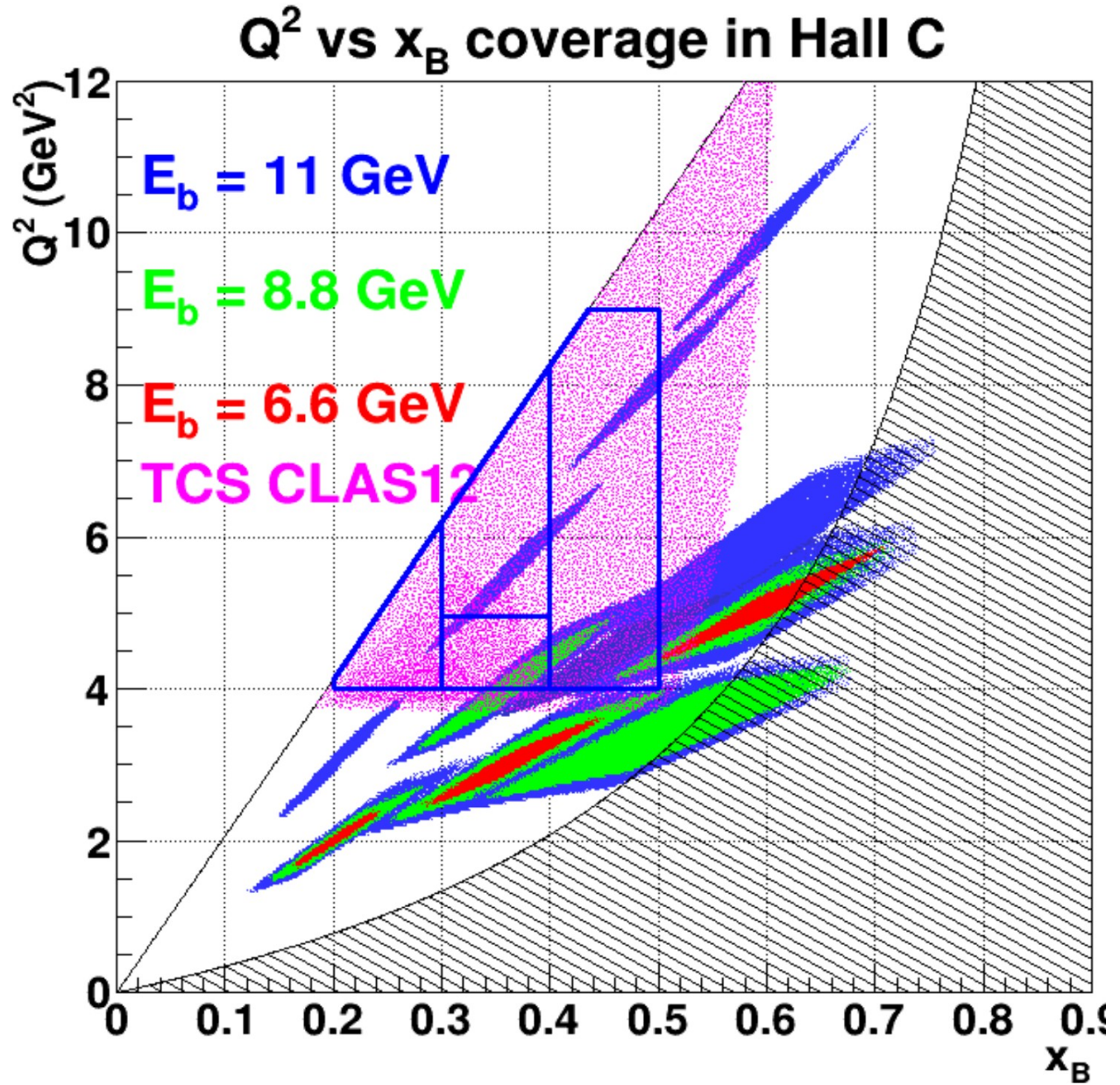


Figure 5: The  $Q^2$  vs  $x_B$  distribution for the approved Hall-C kinematics (blue, green, and red areas), and TCS kinematics with CLAS12 acceptance (pink area).

distribution for the approved Hall-C kinematics (blue, green, and red areas), and TCS kinematics with CLAS12 acceptance (pink area).

In that plot the black solid line corresponds to the maximum achievable  $Q^2$  for a given beam energy. Usually in DVCS experiments maximum  $Q^2$  is not accessible experimentally, since it requires detection of a very low momentum electron, which are usually out of the acceptance, therefore as one can see DVCS kinematic coverage doesn't reach to the maximum accessible  $Q^2$  values. In TCS however maximum  $Q^2$  is well inside the the acceptance region for CLAS12 detector (both leptons are high energy and have large

86 scattering angles).

87 In the fig.5, areas inside solid blue lines are proposed kinematic regions for TCS analysis. In particular  
88 the lowest  $x_B$  region ( $x_B \in (0.2 - 0.3)$ ) can be complementary to DVCS, since this  $Q^2, x_B$  point is not  
89 accessible in any JLab DVCS experiments. Other points can serve as a test of universality of GPDs. I  
90 want to mention that these regions are selected in a way to have roughly equal statistics in all bins, and  
91 in total there was about 6000 expected events in each  $Q'^2, x_B$  bin.

## 92 5 Summary and outlook

93 It was demonstrated here that, the real part of the scattering amplitude  $ReM^{--}$  can be extracted by  
94 fitting the WCRS as a function of  $\phi$  angle. This is somewhat different from the calculation of the cosine  
95 moment which is proposed in paper. [1]. The procedure of estimation of statistical uncertainties is also  
96 discussed.

97 The CLAS(12) acceptance imposes significant  $\phi$  dependent variation of  $\theta$  range, however because of  
98 the known  $\theta$  dependence of the cross section, we can extrapolate the cross section to a fixed range in all  $\phi$   
99 bins, however proper determination of  $\theta$  range needs more studies.

100 Based on old FASTMC code and 120 days of full luminosity, this study chose 4 kinematic bins in  $Q'^2, x_B$   
101 phase space, and the lowest  $x_B$  can serve as a complementary to DVCS program since it has potential  
102 to cover a phase space not accessible in DVCS experiments at JLab. However situation now is different,  
103 and in order to estimate rates more realistically these studies should be repeated with GEMC and be  
104 reconstructed with the current CLAS12 reconstruction code, and we need to use the currently available  
105 luminosity to estimate expected statistics.

## 106 References

- 107 [1] E. R. Berger, M. Diehl and B. Pire, Eur. Phys. J. C **23**, 675 (2002) doi:10.1007/s100520200917  
108 [hep-ph/0110062].
- 109 [2] Slides presented at thw workshop “Deeply Virtual Compton Scattering:  
110 From Observables to GPDs” [http://www.tp2.rub.de/forschung/vortraege-und-](http://www.tp2.rub.de/forschung/vortraege-und-workshops/dvcs2014/program/downloads/paremuzyan.pdf)  
111 [workshops/dvcs2014/program/downloads/paremuzyan.pdf](http://www.tp2.rub.de/forschung/vortraege-und-workshops/dvcs2014/program/downloads/paremuzyan.pdf)
- 112 [3] DVCS Experiment proposal in Hall-C. [https://www.jlab.org/exp\\_prog/proposals/13/PR12-13-](https://www.jlab.org/exp_prog/proposals/13/PR12-13-010.pdf)  
113 [010.pdf](https://www.jlab.org/exp_prog/proposals/13/PR12-13-010.pdf)